

Spin Relaxation Mechanism in Graphene: Resonant Scattering by Magnetic Impurities

Denis Kochan, Martin Gmitra, and Jaroslav Fabian

Institute for Theoretical Physics, University of Regensburg, 93040 Regensburg, Germany

(Received 5 September 2013; published 18 March 2014)

We propose that the observed small (100 ps) spin relaxation time in graphene is due to resonant scattering by local magnetic moments. At resonances, magnetic moments behave as spin hot spots: the spin-flip scattering rates are as large as the spin-conserving ones, as long as the exchange interaction is greater than the resonance width. Smearing of the resonance peaks by the presence of electron-hole puddles gives quantitative agreement with experiment, for about 1 ppm of local moments. Although magnetic moments can come from a variety of sources, we specifically consider hydrogen adatoms, which are also resonant scatterers. The same mechanism would also work in the presence of a strong local spin-orbit interaction, but this would require heavy adatoms on graphene or a much greater coverage density of light adatoms. To make our mechanism more transparent, we also introduce toy atomic chain models for resonant scattering of electrons in the presence of a local magnetic moment and Rashba spin-orbit interaction.

DOI: 10.1103/PhysRevLett.112.116602

PACS numbers: 72.80.Vp, 72.25.Rb

Graphene [1,2] has been considered an ideal spintronics [3,4] material. Its spin-orbit coupling being weak, the spin lifetimes of Dirac electrons are expected to be long, on the order of microseconds [5]. Yet experiments find tenths of a nanosecond [6–13]. This vast discrepancy has been the most outstanding puzzle of graphene spintronics. Despite intense theoretical efforts [14–21], the mechanism for the spin relaxation in graphene has remained elusive. Recently, mesoscopic transport experiments [22] found evidence that local magnetic moments could be the culprits. Here we propose a mechanism of how even a small concentration of such moments can drastically reduce the spin lifetime of Dirac electrons. If the local moments sit at resonant scatterers, such as vacancies [23–25] and adatoms [25,26], they can act as spin hot spots [27]: while contributing little to momentum relaxation, they can dominate spin relaxation. Our mechanism is general, but to obtain quantitative results we use model parameters corresponding to hydrogen adatoms which yield both resonant scattering and local moments [26,28,29]. The calculated spin relaxation rates for 1 ppm of local moments, when averaged over electron density fluctuations due to electron-hole puddles, are in quantitative agreement with experiment. Our theory shows that in order to increase the spin lifetime in graphene, local magnetic moments at resonant scatterers need to be chemically isolated or otherwise eliminated.

In graphene the presence of local magnetic moments is not obvious, unless the magnetic sites (vacancies or adatoms) [30] are intentionally produced [24,25]. It is reasonable to expect that there are not more magnetic sites than, say, 1 ppm, in “clean” graphene samples investigated for spin relaxation in experiments [6–13]. For this concentration a simple estimate gives a weak spin relaxation rate, similar to what is predicted for spin-orbit coupling mechanisms. Indeed, the Fermi golden rule gives, for

exchange coupling J between electrons and local moments, spin relaxation rate $1/\tau_s \approx (2\pi/\hbar)\eta J^2 \nu_0(E_F)$, where $\nu_0(E_F)$ is graphene’s density of states at the Fermi level and η is the concentration of the moments. Taking representative values of $J \approx 0.4$ eV, $\eta \approx 10^{-6}$, and $E_F \approx 0.1$ eV (for which ν_0 is about 0.01 states per eV and atom), one gets spin relaxation times of 100 ns, 3 orders below the experimental 100 ps.

We show here that the spin relaxation due to magnetic impurities in graphene is significantly enhanced by resonant scattering, for which the perturbative Fermi golden rule does not apply. The intuitive idea is that if the exchange coupling energy J is greater than the resonant energy width Γ , the electron spin can precess at the resonant site during the interaction time \hbar/Γ with the impurity of a significant fraction of its spin precession period \hbar/J . Then the spin-flip probability becomes as likely as the spin-conserving one, as in spin hot spots [27]. This idea is quantitatively confirmed by an explicit calculation on graphene with a chemisorbed hydrogen adatom [31,32], which produces resonances near the graphene neutrality point [28,33] and induces magnetic moments [25,26]. We add exchange coupling to the adatom model [28] and calculate the T-matrix and spin relaxation rate. We also introduce toy models—electrons hopping on one-dimensional atomic chains with resonant quantum wells—and analyze two competitive spin relaxation mechanisms—scattering off a magnetic moment and Rashba spin-orbit coupling. For realistic strengths of adatom induced exchange and Rashba couplings in graphene, the former dominates.

To investigate the local magnetic moments (as has been done earlier [26]) we perform a supercell first-principles band structure calculation. Details about parametrization of the band structure in terms of local effective exchange couplings and their realistic estimates are summarized in [34].

Resonant scattering by magnetic impurities.—To solve the magnetic scattering problem in the single impurity limit in graphene we add to the graphene Hamiltonian $H_0 = -t\sum_{\langle m,n \rangle} c_m^\dagger c_n$ ($t = 2.6$ eV) the following interaction term:

$$H(\hat{\mathbf{S}}) = \sum_{\sigma} \varepsilon_h h_{\sigma}^{\dagger} h_{\sigma} + T(h_{\sigma}^{\dagger} c_{C_H, \sigma} + c_{C_H, \sigma}^{\dagger} h_{\sigma}) - J\hat{\mathbf{S}} \cdot \hat{\mathbf{S}}. \quad (1)$$

Here, h_{σ}^{\dagger} (h_{σ}) and c_{σ}^{\dagger} (c_{σ}) are fermionic creation (annihilation) operators acting on the adatom and graphene carbon sites, respectively, and the subscript $\sigma = -\bar{\sigma} = \{\uparrow, \downarrow\}$ stands for the spin component along the z direction (quantization axis). The first two terms express on-site and hybridization energies, respectively, that couple the adatom (in our case hydrogen H) to a graphene host at a carbon site C_H . The last term in Eq. (1) is the exchange interaction between the electron spin $\hat{\mathbf{S}}$ on the hydrogen (resonant site) and the intrinsic impurity moment $\hat{\mathbf{S}}$. Here $\hat{\mathbf{s}}$ and $\hat{\mathbf{S}}$ stand for Pauli spin one-half matrices and not for spin operators. Orbital parameters for the chemisorbed hydrogen were fitted already in Ref. [29], $\varepsilon_h = 0.16$ eV and $T = 7.5$ eV, and for the exchange we take $J = -0.4$ eV. This value is consistent with a more detailed parametrization of the magnetic impurity model [34]. The precise value of J is not really important. First, the spin relaxation rates, when broadened by puddles, are hardly influenced by J as long as $J \gg \Gamma$ [34]. Second, in graphene, additionally other adatoms or vacancies give magnetic moments, so that eventually one would need to average over the ranges of adatom hopping and exchange parameters (we lump this averaging under puddle broadening).

In the independent electron-impurity picture (we do not discuss Kondo physics), the total Hamiltonian $H_0 + H(\hat{\mathbf{S}})$ diagonalizes in the singlet ($\ell = 0$) and triplet ($\ell = 1$) basis $|\ell, m_{\ell}\rangle$ (here m_{ℓ} runs from $-\ell$ to ℓ). Eliminating by downfolding (Löwdin transformation) H orbitals, we arrive at the single-site impurity Hamiltonian,

$$H_{\text{fold}}(\hat{\mathbf{S}}) = \sum_{\ell, m_{\ell}} \alpha_{\ell}(E) c_{C_H, \ell, m_{\ell}}^{\dagger} c_{C_H, \ell, m_{\ell}}, \quad (2)$$

where the energy-dependent on-site coupling is

$$\alpha_{\ell}(E) = \frac{T^2}{E - \varepsilon_h + (4\ell - 3)J}, \quad (3)$$

different for the singlet and triplet states.

The T-matrix elements for the above impurity problem can be calculated as (see, e.g., [35])

$$\mathbb{T}(E)_{\kappa', \ell', m_{\ell'} | \kappa, \ell, m_{\ell}} = \frac{1}{N_C} \frac{\delta_{\ell, \ell'} \delta_{m_{\ell}, m_{\ell'}} \alpha_{\ell}(E)}{1 - \alpha_{\ell}(E) G_0(E)}, \quad (4)$$

where κ labels the momentum and band index of graphene's Bloch states, N_C is the number of carbon

sites in the sample, and $G_0(E)$ is the retarded Green function per carbon atom and the spin of unperturbed graphene. Near the neutrality point ($E = 0$), $G_0(E) \simeq \frac{E}{D^2} [\ln |E^2/D^2 - E^2| - i\pi \text{sgn}(E) \Theta(D - |E|)]$, where the graphene bandwidth is $D = \sqrt{\sqrt{3}\pi}t \approx 6$ eV.

Resonant states appear for energies $|E| < D$ at which the real part of the denominator of Eq. (4) equals zero. Near the neutrality point ($|E| \ll D$) we get the equation

$$E_{\text{res}, \ell} \left(1 - \frac{T^2}{D^2} \ln \frac{E_{\text{res}, \ell}^2}{D^2} - \frac{T^2}{D^4} E_{\text{res}, \ell}^2 \right) = \varepsilon_h - (4\ell - 3)J, \quad (5)$$

which determines the resonant energies $E_{\text{res}, \ell}$ for the singlet and triplet states. For a nonmagnetic impurity ($J = 0$) there appears a single resonant level close to the neutrality point [28]. For a magnetic impurity this level splits to singlet and triplet peaks, and shifts in energy. For $J < 0$ the singlet resonance has a lower energy; see [34].

From the T-matrix we obtain a spin-flip rate $1/\tau_s$ at zero temperature (thermal broadening is discussed in [34]),

$$1/\tau_s = \eta \frac{2\pi}{\hbar} \nu_0(E) f_{\sigma, \bar{\sigma}} \left[\frac{\alpha_1(E)}{1 - \alpha_1 G_0(E)}, \frac{\alpha_0(E)}{1 - \alpha_0 G_0(E)} \right], \quad (6)$$

for the fraction of $\eta = N_H/N_C$ of impurities per carbon atom, for which we assume a zero net spin polarization. Couplings $\alpha_{\ell}(E)$ are given by Eq. (3), $G_0(E)$ and $\nu_0(E)$ are graphene's Green function and DOS per atom and spin. The auxiliary function $f_{\sigma, \sigma'}[x, y]$ entering Eq. (6),

$$f_{\sigma, \sigma'}[x, y] = \frac{1}{2} \delta_{\sigma, \sigma'} |x|^2 + \frac{1}{8} |x + (\sigma \cdot \sigma')y|^2, \quad (7)$$

originates from a probability decomposition of a particular spin-flip process: $\sigma + \Sigma_{\text{imp}} \rightarrow \sigma' + \Sigma'_{\text{imp}}$ in terms of singlet and triplet transitions. The spin-flip rate $1/\tau_s$ is peaked at resonances where denominators $1 - \alpha_{\ell}(E)G_0(E)$ have minima.

The spin relaxation rate $1/\tau_s$ is plotted in Fig. 1, which is the main result of this Letter. The zero temperature rate shows singlet and triplet split resonance peaks, with widths Γ of about 20 and 40 meV, respectively. At 300 K the peaks merge. In realistic samples the neutrality point fluctuates due to electron-hole puddles [36,37]. Also, different magnetic impurities would give different peak positions and widths, providing additional broadening. All such effects are modeled by phenomenological Gaussian energy broadening with standard deviation σ_{br} . In Fig. 1 we use $\sigma_{\text{br}} = 110$ meV. From Fig. 1(b) we can conclude that the temperature dependence of $1/\tau_s$ is rather weak, essentially given by Fermi broadening of the resonance structure. Finally, in Fig. 1(c) we compare the calculated spin relaxation rates with experiment, with adjusted η . The agreement is remarkable. In fact, one can find a nice

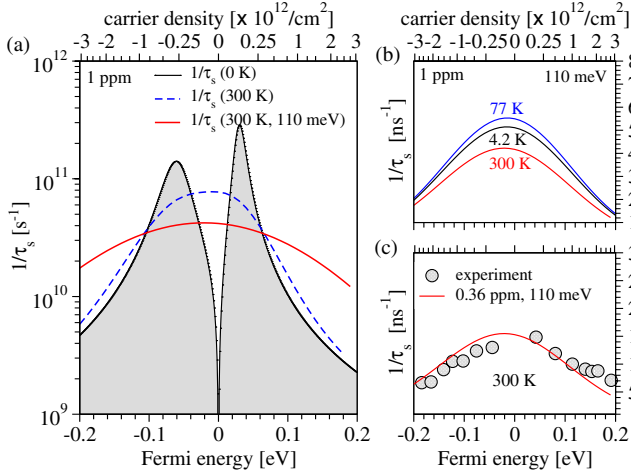


FIG. 1 (color online). Resonant enhancement of spin relaxation in graphene. Exchange coupling $J = -0.4$ eV and impurity fraction η in ppm is indicated. (a) Spin relaxation rate $1/\tau_s$ as a function of energy-carrier density, at 0 K, at 300 K, and at 300 K broadened by puddles with energy fluctuations of 110 meV. (b) Broadened $1/\tau_s$ at different temperatures. (c) Comparison between theory and experiment (graphene data from Ref. [38]) at 300 K.

agreement for a large window of J (see [34]) by adjusting σ_{br} and η . Vacancies and different adatoms are well covered by this mechanism.

In [34] we plot $1/\tau_s$ for ferromagnetic $J = 0.4$ eV. The only effect, after broadening, is the opposite (slight) skewness of the energy dependence (keeping ε_h unchanged), coming from the flipped positions of the singlet and triplet peaks. Also, in [34] we demonstrate that resonance enhancement of $1/\tau_s$ is present for even much smaller J , as long as $J \gtrsim \Gamma$, confirming the intuitive picture of the enhancement coming from the spin precession being faster than the leakage rate. One important conclusion can be drawn from this concerning spin-orbit coupling (SOC). Hydrogen adatoms induce SOC of about 1 meV [29,39]. Assuming it is located on resonant site, this is smaller than $\Gamma \approx 20$ meV, so the resonant spin-orbit enhancement will be much less pronounced, unless η is increased to, say 10^{-3} , see [34] and the 1D model below. Nevertheless, there could be heavier adatoms that induce both large spin-orbit coupling and resonant scattering so that resonance enhancement could be present. It was recently shown that Si adatoms sitting on top of the carbon bridge positions could also give 100 ps spin-flip times [21], but for concentrations of $\eta \sim 10^{-3}$, 3 orders more than what is needed for magnetic resonant scatterers. It is possible that the mechanism is indeed resonance enhancement of the spin-flip rates due to induced spin-orbit coupling. In fact, resonant scattering by impurities induced SOC was already invoked to explain strong spin-flip scattering in alkali [40] and noble [41] metals.

There have already been spin relaxation experiments with hydrogenated graphene. According to our theory, an

sp^3 bonded hydrogen should increase the spin relaxation rate. Unfortunately, the experimental results differ. In Ref. [38] the spin relaxation rate decreased upon hydrogenation. In Ref. [39] spin relaxation has not changed much, while in Ref. [25] evidence for magnetic moments was provided based on a different model, that of fluctuating magnetic fields. It is likely that the experimental outcomes depend on the hydrogenation method. At present it is not possible to form a unique experimental picture with which we could gauge our theory. But we stress that we use hydrogen only as a convenient model to formulate our mechanism quantitatively. The Hamiltonian we use is rather generic, and the results are very robust as far as the details in J and other parameters are concerned. It is even possible that hydrogenation isolates existing magnetic moments at vacancies, thereby increasing τ_s , as seen in Ref. [38].

Resonant spin-flip scattering in a one-dimensional double-barrier atomic chain.—To make the resonant enhancement of the spin relaxation rate more transparent, we introduce a toy model that captures all the essential features. Consider an atomic chain with lattice constant b , whose central site ($m = 0$), trapped within two δ barriers on its nearest neighbors, hosts the exchange interaction $-J\hat{s} \cdot \hat{S}$. The hopping Hamiltonian is

$$H = -t \sum_{\langle m,n \rangle} (c_m^\dagger c_n + c_n^\dagger c_m) + U \sum_{m=\mp 1} c_m^\dagger c_m - J\hat{s} \cdot \hat{S}, \quad (8)$$

as sketched in the inset of Fig. 2(a). In the singlet-triplet basis the transmission and reflection amplitudes $\gamma_{\ell,m_\ell}(k)$ and $\beta_{\ell,m_\ell}(k)$, are obtained analytically as

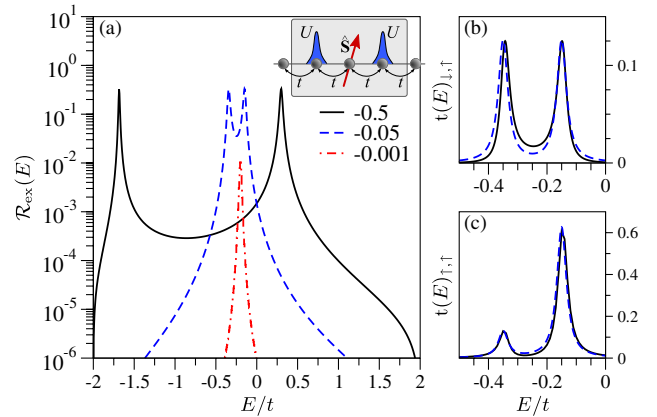


FIG. 2 (color online). Resonant enhancement of spin flips in a one-dimensional atomic chain with a double barrier hosting an impurity spin. (a) Ratio $\mathcal{R}_{ex}(E)$ of spin-flip and spin-conserving transition probabilities for $U/t = 10$ and indicated J/t . The inset shows the model. (b) Spin-flip $t(E)_{l,r}$ and (c) spin-conserving $t(E)_{l,r}$ probabilities for $J/t = -0.05$. The solid lines are exact formulas, Eqs. (11)–(12), the dashed lines are approximations, Eq. (13).

$$\gamma_{\ell, m_\ell} = \frac{2it(1 + Ue^{ikb}/t)^{-1} \sin(kb)}{[E_k + J(4\ell - 3)](1 + Ue^{ikb}/t) + 2te^{ikb}}, \quad (9)$$

$$\beta_{\ell, m_\ell} = \gamma_{\ell, m_\ell}(k) - \frac{t + Ue^{-ikb}}{t + Ue^{ikb}}. \quad (10)$$

The energy of the incident electron of momentum k is $E_k = -2t \cos(kb)$, and the composite (electron and impurity) spin state $|\ell, m_\ell\rangle$ corresponds to singlet ($\ell = 0$) and triplet ($\ell = 1$), with the angular momentum projection m_ℓ (this index is dropped in what follows, as neither amplitude depends on it). We are interested in the transmission $t = |\gamma|^2$ and reflection $r = |\beta|^2$ probabilities of various spin transition processes $\sigma \rightarrow \sigma'$ so we trace out the impurity spin. The result is

$$t(E_k)_{\sigma, \sigma'} = f_{\sigma, \sigma'}[\gamma_1(k), \gamma_0(k)], \quad (11)$$

$$r(E_k)_{\sigma, \sigma'} = f_{\sigma, \sigma'}[\beta_1(k), \beta_0(k)], \quad (12)$$

where the function $f_{\sigma, \sigma'}$ is given by Eq. (7). The above results are shown in Fig. 2(a). We plot the ratio $\mathcal{R}_{\text{ex}}(E)$ of spin flip versus spin-conserving probabilities $\mathcal{R}_{\text{ex}}(E) = [t(E)_{\sigma, \bar{\sigma}} + r(E)_{\sigma, \bar{\sigma}}]/[t(E)_{\sigma, \sigma} + r(E)_{\sigma, \sigma}]$ for different values of the exchange strength J/t . For $J/t = -0.5$ and -0.05 , i.e., when $t^2/U^2 \lesssim J/t$, spin-flip transitions are as likely as the spin-conserving ones. For smaller J/t , spin-flip probabilities become proportional to J^2 , reaching the usual perturbative regime.

Pronounced resonances appear for $U \gg t$. In this limit the singlet and triplet resonant energies are $E_{\text{res}, \ell} \approx -2t^2/U - J(4\ell - 3)$, and $\Gamma \approx t^3/4U^2$ is the resonance width. The dwell time $\Delta t_{\text{dw}} = \hbar/\Gamma$ is much greater than the hopping time \hbar/t . We further assume that $\Gamma \lesssim J$, which is the limit of resonant enhancement of the spin relaxation rate. This condition means that the electron has enough time to precess by the exchange field before leaking out of the well. The singlet and triplet resonance peaks are well resolved in this limit. Equation (11) now gives the Lorentzian,

$$t(E)_{\sigma, \sigma'} \approx \sum_{\ell=0,1} \frac{(4\ell \delta_{\sigma, \sigma'} + 1)t^6/2U^4}{(E - E_{\text{res}, \ell})^2 + 4t^6/U^4}, \quad (13)$$

and, similarly, Eq. (12) for the reflectivities; $r_{\sigma, \bar{\sigma}} = t_{\sigma, \bar{\sigma}}$, and $r_{\sigma, \sigma} = 1 - r_{\sigma, \bar{\sigma}} - t_{\sigma, \sigma} - t_{\sigma, \bar{\sigma}}$. Figures 2(b) and 2(c) show the comparison of the exact and above approximative formulas for $J/t = -0.05$. The peak positions depend on J via $E_{\text{res}, \ell}$, but the values at maxima are J independent. At resonances the spin-flip to spin-conserving probabilities come as 1/3—see Fig. 2(a)—25% of the scattered electrons change spin. The reason is that a spin-up electron forms a triplet state $|1, 1\rangle$ with a 50% chance, $|1, 0\rangle$ and $|0, 0\rangle$ with a 25% chance. The chance that the electron flips its spin is 50% for each $|1, 0\rangle$ and $|0, 0\rangle$ states. This gives a 25% probability for a spin flip, as we see at resonances.

In [34] we show, using our 1D model, that an impurity sitting at the barrier site and not on the resonant site inside the well, does not have such a pronounced effect on the spin-flip probability. This justifies our resonant-site-centered exchange model of magnetic impurity on graphene.

Resonant spin-orbit scattering in a one-dimensional double-barrier atomic chain.—Consider the Hamiltonian in Eq. (8) with the exchange interaction substituted by the one-dimensional Rashba-like spin-orbit coupling

$$H_R = \lambda \sum_{m=\mp 1} \sum_{\sigma} (\sigma m) [c_{m, \sigma}^\dagger c_{0, \bar{\sigma}} + c_{0, \bar{\sigma}}^\dagger c_{m, \sigma}], \quad (14)$$

which is spin-flip hopping between the barrier sites at $m = \pm 1$ and the central site at $m = 0$. Assuming an incident electron with momentum k , energy $E_k = -2t \cos(kb)$, and spin polarization σ , the reflection spin-flip amplitude $\beta_{\sigma, \bar{\sigma}}$ is identically zero and the remaining ones are

$$\gamma_{\sigma, \sigma'} = \left[\left(1 - \frac{\lambda^2}{t^2} \right) \delta_{\sigma, \sigma'} + 2 \frac{\lambda}{t} \delta_{\bar{\sigma}, \sigma'} \right] M(k), \quad (15)$$

$$\beta_{\sigma, \sigma} = \left[-e^{-2ikb} + \left(e^{-2ikb} - \frac{\lambda^2}{t^2} - \frac{U}{t} E_k \right) M(k) \right], \quad (16)$$

where the auxiliary function $M(k)$ reads

$$M(k) = \frac{2it(1 + Ue^{ikb}/t)^{-1} \sin(kb)}{E_k(1 + Ue^{ikb}/t) + 2\lambda^2 e^{ikb}/t + 2te^{ikb}}. \quad (17)$$

The above results are visualized in Fig. 3(a). We plot the ratio $\mathcal{R}_{\text{soc}}(E)$ of spin-flip versus spin-conserving probabilities $\mathcal{R}_{\text{soc}}(E) = [|\gamma_{\sigma, \bar{\sigma}}|^2 + |\beta_{\sigma, \bar{\sigma}}|^2]/[|\gamma_{\sigma, \sigma}|^2 + |\beta_{\sigma, \sigma}|^2]$ for different values of spin-orbit coupling strength λ/t in the resonant limit, i.e., when $U \gg t$. Numerical values of

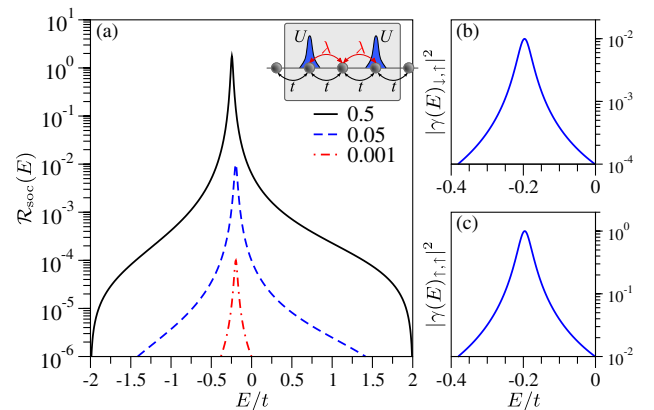


FIG. 3 (color online). Resonant spin-orbit coupling mechanism of spin relaxation processes in a one-dimensional atomic chain with a double barrier with Rashba SOC. (a) Ratio $\mathcal{R}_{\text{soc}}(E)$ of spin-flip and spin-conserving transition probabilities for $U/t = 10$ and indicated values of λ/t . (b) Spin-flip $|\gamma(E)_{\downarrow, \uparrow}|^2$ and (c) spin-conserving $|\gamma(E)_{\uparrow, \uparrow}|^2$ probabilities for $\lambda/t = 0.05$.

$\lambda/t = 0.001, 0.05, 0.5$, taken to compare with Fig. 2, roughly correspond to hydrogenated graphene [29,39], fluorinated graphene [42], and graphene with thallium [43]. In all three cases there is a pronounced enhancement of spin relaxation close to the resonant energy $-2t^2/U$. However, comparison of $\mathcal{R}_{\text{ex}}(E)$ and $\mathcal{R}_{\text{soc}}(E)$, Figs. 2(a) and 3(a), show that unless SOC is very strong, the resonant exchange mechanism dominates over the spin-orbit one.

In conclusion, we propose that resonant scattering by magnetic impurities in graphene causes the observed fast spin relaxation rates. Resonant enhancement of the exchange interaction, but also of the weaker spin-orbit coupling, opens new prospects for investigating impurity magnetic moments, dynamical polarization of impurity spins, Kondo physics, and resonant scattering in graphene. The mechanism, via the presented toy models of 1D electron hopping, could also be potentially realized with ultracold fermi gases.

We thank T. Wehling for useful discussions, T. Maassen for providing us the experimental data for Fig. 1, and P. Mavropoulos for useful discussions and for pointing to us Ref. [40]. This work was supported by the DFG SFB 689, SPP 1285 and the European Union Seventh Framework Programme under Grant Agreement No. 604391 Graphene Flagship.

-
- [1] A. K. Geim and K. S. Novoselov, *Nat. Mater.* **6**, 183 (2007).
 [2] A. H. Castro Neto, *Science* **332**, 315 (2011).
 [3] I. Žutić, J. Fabian, and S. Das Sarma, *Rev. Mod. Phys.* **76**, 323 (2004).
 [4] J. Fabian, A. Matos-Abiad, C. Ertler, P. Stano, and I. Žutić, *Acta Phys. Slovaca* **57**, 565 (2007).
 [5] D. Pesin and A. H. MacDonald, *Nat. Mater.* **11**, 409 (2012).
 [6] N. Tombros, C. Józsa, M. Popinciuc, H. T. Jonkman, and B. J. van Wees, *Nature (London)* **448**, 571 (2007).
 [7] N. Tombros, S. Tanabe, A. Veligura, C. Józsa, M. Popinciuc, H. T. Jonkman, and B. J. van Wees, *Phys. Rev. Lett.* **101**, 046601 (2008).
 [8] K. Pi, W. Han, K. M. McCreary, A. G. Swartz, Y. Li, and R. K. Kawakami, *Phys. Rev. Lett.* **104**, 187201 (2010).
 [9] T.-Y. Yang, J. Balakrishnan, F. Volmer, A. Avsar, M. Jaiswal, J. Sann, S. R. Ali, A. Pachoud, M. Zeng, M. Popinciuc, G. Güntherodt, B. Beschoten, and B. Özyilmaz, *Phys. Rev. Lett.* **107**, 047206 (2011).
 [10] W. Han and R. K. Kawakami, *Phys. Rev. Lett.* **107**, 047207 (2011).
 [11] A. Avsar, T.-Y. Yang, S. Bae, J. Balakrishnan, F. Volmer, M. Jaiswal, Z. Yi, S. R. Ali, G. Güntherodt, B. H. Hong, B. Beschoten, and B. Özyilmaz, *Nano Lett.* **11**, 2363 (2011).
 [12] S. Jo, D.-K. Ki, D. Jeong, H.-J. Lee, and S. Kettemann, *Phys. Rev. B* **84**, 075453 (2011).
 [13] R. G. Mani, J. Hankinson, C. Berger, and W. A. de Heer, *Nat. Commun.* **3**, 996 (2012).
 [14] D. Huertas-Hernando, F. Guinea, and A. Brataas, *Phys. Rev. B* **74**, 155426 (2006).
 [15] B. Dora, F. Muranyi, and F. Simon, *Europhys. Lett.* **92**, 17002 (2010).
 [16] J.-S. Jeong, J. Shin, and H.-W. Lee, *Phys. Rev. B* **84**, 195457 (2011).
 [17] V. K. Dugaev, E. Y. Sherman, and J. Barnaś, *Phys. Rev. B* **83**, 085306 (2011).
 [18] C. Ertler, S. Kunschuh, M. Gmitra, and J. Fabian, *Phys. Rev. B* **80**, 041405 (2009).
 [19] P. Zhang and M. W. Wu, *Phys. Rev. B* **84**, 045304 (2011).
 [20] H. Ochoa, A. H. Castro Neto, and F. Guinea, *Phys. Rev. Lett.* **108**, 206808 (2012).
 [21] D. V. Fedorov, M. Gradhand, S. Ostanin, I. V. Maznichenko, A. Ernst, J. Fabian, and I. Mertig, *Phys. Rev. Lett.* **110**, 156602 (2013).
 [22] M. B. Lundeberg, R. Yang, J. Renard, and J. A. Folk, *Phys. Rev. Lett.* **110**, 156601 (2013).
 [23] M. M. Ugeda, I. Brihuega, F. Guinea, and J. M. Gomez-Rodriguez, *Phys. Rev. Lett.* **104**, 096804 (2010).
 [24] R. R. Nair, M. Sepioni, I. L. Tsai, O. Lehtinen, J. Keinonen, A. V. Krasheninnikov, T. Thomson, A. K. Geim, and I. V. Grigorieva, *Nat. Phys.* **8**, 199 (2012).
 [25] K. M. McCreary, A. G. Swartz, W. Han, J. Fabian, and R. K. Kawakami, *Phys. Rev. Lett.* **109**, 186604 (2012).
 [26] O. Yazyev, *Rep. Prog. Phys.* **73**, 056501 (2010).
 [27] J. Fabian and S. Das Sarma, *Phys. Rev. Lett.* **81**, 5624 (1998).
 [28] T. O. Wehling, S. Yuan, A. I. Lichtenstein, A. K. Geim, and M. I. Katsnelson, *Phys. Rev. Lett.* **105**, 056802 (2010).
 [29] M. Gmitra, D. Kochan, and J. Fabian, *Phys. Rev. Lett.* **110**, 246602 (2013).
 [30] B. Uchoa, V. N. Kotov, N. M. R. Peres, and A. H. Castro Neto, *Phys. Rev. Lett.* **101**, 026805 (2008).
 [31] C. Elias, R. R. Nair, T. M. G. Mohiuddin, S. V. Morozov, P. Blake, M. P. Halsall, A. C. Ferrari, D. W. Boukhvalov, M. I. Katsnelson, A. K. Geim, and K. S. Novoselov, *Science* **323**, 610 (2009).
 [32] D. Haberer, D. V. Vyalikh, S. Taioli, B. Dora, M. Farjam, J. Fink, D. Marchenko, T. Pichler, K. Ziegler, S. Simonucci, M. S. Dresselhaus, M. Knupfer, B. Büchner, and A. Grüneis, *Nano Lett.* **10**, 3360 (2010).
 [33] B. R. Matis, B. H. Houston, and J. W. Baldwin, *Phys. Rev. B* **88**, 085441 (2013).
 [34] See Supplemental Material at <http://link.aps.org/supplemental/10.1103/PhysRevLett.112.116602> for details on *ab-initio* calculations, thermal broadening, and spin-relaxation rates for various weakened exchange-coupling strengths.
 [35] A. C. Hewson, *The Kondo Problem to Heavy Fermions* (Cambridge University Press, Cambridge, England, 1993).
 [36] E. H. Hwang, S. Adam, and S. Das Sarma, *Phys. Rev. Lett.* **98**, 186806 (2007).
 [37] A. Deshpande, W. Bao, F. Miao, C. N. Lau, and B. J. LeRoy, *Phys. Rev. B* **79**, 205411 (2009).
 [38] M. Wojtaszek, I. J. Vera-Marun, T. Maassen, and B. J. van Wees, *Phys. Rev. B* **87**, 081402 (2013).
 [39] J. Balakrishnan, G. K. W. Koon, M. Jaiswal, A. H. Castro Neto, and B. Özyilmaz, *Nat. Phys.* **9**, 284 (2013).
 [40] S. D. Mahanti and F. Toigo, *Phys. Lett.* **36A**, 61 (1971).
 [41] Phivos Mavropoulos (private communication).
 [42] S. Irmer, T. Frank, D. Kochan, M. Gmitra, and J. Fabian (unpublished).
 [43] C. Weeks, J. Hu, J. Alicea, M. Franz, and R. Wu, *Phys. Rev. X* **1**, 021001 (2011).